MACEIÓ - ALAGOAS
EBA 15
15° ENCONTRO BRASILEIRO SOBRE ADSORÇÃO
15th Brazilian Meeting about Adsorption

Copper and Iron Sulfides in Hydroxyapatite Adsorbents for Mercury Immobilization

Megale, E. Z.[a], Martins., N[b], Camargo, C.L.M[b], Resende, N. S. de[a], Salim, V. M. M.[a]

[a] *Chemical Engineering Program (PEQ/COPPE) - Universidade Federal do Rio de Janeiro, Cidade Universitária, Rio de Janeiro 21941-972, Brazil*
[b] *Escola de Química - Universidade Federal do Rio de Janeiro, Cidade Universitária, Rio de Janeiro 21941-972, Brazil*

Abstract

The main source of gaseous elemental mercury emissions in South America is artisanal gold mining, where emissions reach 340 tons/year. Numerous studies have reported chronic exposure of the Amazon region's population to mercury through inhalation and ingestion. Furthermore, deforestation and recurrent wildfires increase mercury mobility in that region, magnifying population intoxication. The objective was to develop adsorbents containing metal sulfides dispersed in hydroxyapatite. The synthesis methods used to prepare the adsorbents were coprecipitation, ion exchange, and activation via sulfidation. X-ray fluorescence (XRF), X-ray diffraction (XRD), and N_2 adsorption/desorption at 77 K were used for physicochemical characterization, and the adsorption capacity was analyzed through batch adsorption tests at room temperature. The mass content of iron and copper varied between 4.6% w/w to 15% w/w, and high specific areas were obtained between 79.4 to 166.1 m^2/g. The adsorption capacity of iron sulfide-hydroxyapatite was 145.6 mg/g, while copper sulfide-hydroxyapatite was 197.7 mg/g. Pure hydroxyapatite adsorbed amounts ranging from 0.7 mg/g to 2.2 mg/g. In addition, the mercury adsorbed is immobilized until 110 °C. Therefore, a highly effective adsorbent was synthesized by modifying hydroxyapatite with metal sulfides, with a high mass content of the added metals.

Keywords: mercury, copper sulfide, iron sulfide, hydroxyapatite.

1. Introduction

Mercury is an extremely volatile metal with low solubility, making its release into the environment particularly challenging to control [1]. This pollutant is emitted through both natural processes as well as human activities, with the latter increasing in recent years [2]. The primary sources of anthropogenic emissions into the atmosphere are fossil fuel combustion and artisanal and small-scale gold mining, with mining alone accounting for 38% of global emissions. Notably, the Amazon region is responsible for 80% of mercury emissions in South America. [3].

Research on adsorbent properties is increasingly focused on developing materials with higher selectivity, adsorption capacity, stability, and minimal generation of new contaminated residues, all aimed at reducing environmental impact [2].

This work proposes adsorbent development, composed of iron sulfide and copper sulfide dispersed in hydroxyapatite. These two metal sulfides exhibit a high affinity for mercury, forming stable mercury sulfides [4]. Additionally, the physicochemical properties of the adsorbents were analyzed, and batch adsorption assays were conducted to evaluate their efficacy in mercury removal and stabilization.

2. Methodology

2.1 Adsorbents Synthesis

Iron and copper substituted hydroxyapatites [$Ca_{(10-x)}M_x(PO4)_6(OH)_2$, M=Cu or Fe] were synthesized by the co-precipitation method [5,6]. 150 mL of a 0.5M solution of $Ca(NO_3)_2.4H_2O$ and $Fe(NO_3)_3.9H_2O$ or $Cu(NO_3)_2.4H_2O$ was slowly

added with a pH of 10 using a peristaltic pump (1.25 mL/min) into 150 mL of a 0.3M solution of $(NH_4)2HPO_4$. The pH was maintained between 10 and 11 by the addition of NH_4OH. The mixture was kept under constant stirring and at a temperature of 80 °C for 2 hours. After aging, the solid material was separated from the solution by filtration, washed with hot water, dried in an oven at 100 °C for 24 hours, and calcined under an N_2 flow (40 mL/min) at 300 °C for 4 h. This method yielded the samples 4.6CuHap, 8FeHap, and 15FeHap.

To increase the copper content, 3 g of the sample synthesized by co-precipitation (4.6CuHap) were placed in a Becker with 40 mL of a 0.15 M solution of $Cu(NO_3)_2.4H_2O$. This suspension was stirred for 24 hours at room temperature. The resulting material was then filtered, dried, ground, and calcined under the same conditions as the previous step, obtaining the sample 12.6CuHap.

The adsorbent activation was carried out via sulfidation, under 5% H_2S/He flow (40 mL/min) at 350 °C for 2 hours.

2.2 Physicochemical characterization

The chemical composition of the samples was determined by X-ray Fluorescence (XRF) using Rigaku Primini equipment with a Palladium X-ray source. X-ray diffraction (XRD) analyses were conducted in a scan range of $10° \leq 2\theta \leq 80°$ with a step size of 0.02°/5s using a Rigaku Nex De equipment with a graphite monochromator and CuKα radiation (40 kV and 20 mA). The crystallinity study of the material was performed through Rietveld Refinement, using the software FullProf. Textural properties were evaluated by N_2 adsorption/ desorption at 77 K using Micrometrics ASAP 2020 equipment. A high-resolution transmission electron microscope (JEOL 2100F 200kV) was used to evaluate the morphology of adsorbents. The mercury content after adsorption tests was determined using an atomic absorption spectrometer with Zeeman correction (RA-815+, Lumex).

2.3 Adsorption experiments

The adsorption capacity was evaluated in triplicate on batch adsorption experiments performed in a sealed glass container. The container has a bed of mercury (45 mL) and glass support, used to expose the samples to a mercury atmosphere in thermodynamic equilibrium (18,000 and 28,000 μg/m³) for 5, 10, and 20 days.

Mercury temperature-programmed desorption (Hg-TPD) experiments were performed as a function of temperature to evaluate the immobilization capacity of synthesized adsorbents. First, the exhausted adsorbents were under a constant flow of inert gas (20 mL/min) at 40 °C for 20 min. Then, a heating ramp (10 °C/min) to 350 °C was applied.

Results and Discussions

3.1 Physicochemical characteristics of adsorbents

The chemical composition (wt%) and stoichiometric element ratios determined by XRF analysis are listed in Table 1. A Ca/P molar ratio of less than 1.67 indicates the formation of calcium-deficient hydroxyapatite, which was observed in all samples. In the samples modified with iron, the (Ca+Fe)/P ratio approached 1.67, indicating the successful incorporation of Fe^{3+} in the material through the co-precipitation method. Conversely, samples modified with copper using the co-precipitation method exhibited a (Ca+Cu)/P ratio below 1.67. To address this, the copper content was enhanced via the ion exchange method, increasing %Cu from 4.6 to 12.6 %wt.

Table 1. XRF results of the adsorbent's precursors.

Samples	M (wt%)	Ca/P	(Ca+M)/P
4.6CuHap	4.6	1.40	1.52
12.6CuHap	12.6	1.29	1.63
8FeHap	8.0	1.44	1.69
15FeHap	15.0	1.31	1.81

Micrographs indicated that the adsorbents exhibit a needle-like morphology. The N_2 adsorption/ desorption results, presented in Table 2, reveal differences in the textural properties of the copper-modified hydroxyapatite before and after the ion exchange process. A decrease was observed in specific surface area values (S_{BET}) likely attributed to the ion exchange step. In contrast, the samples modified with iron ions showed increased specific surface area and decreased average pore diameter (dp).

Table 2. Textural properties of the adsorbent's precursors.

Samples	S_{BET} (m^2/g)	Vp (cm^3/g)	dp (nm)
4.6CuHap	125.6	0.5	16.3
12.6CuHap	79.4	0.3	17.1
8FeHap	164.2	0.6	16.3
15FeHap	166.1	0.6	14.1

The variation in textural properties can significantly influence the performance of the adsorbents in Hg° removal, as it affects the accessibility of the active sites [7,8]. The XRD results (Yobs) of copper and iron substituted hydroxyapatite (4.6CuHap, 12.6CuHap, 8FeHap, and 15FeHap) and the sulfited adsorbents (12.6CuxSyHap, 8FexSyHap, and 15FexSyHap) are shown in Figure 1.

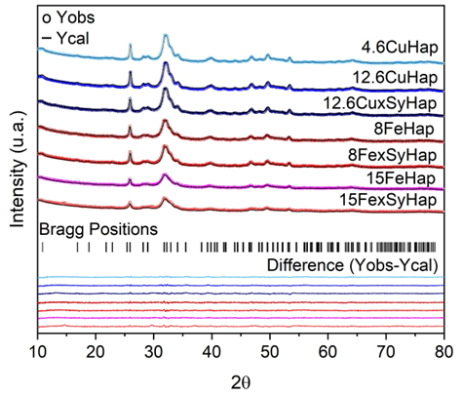

Figure 1. Experimental XRD patterns (Yobs), Rietveld refinement results (Ycalc), and differences between observed and calculated intensity (Yobs-Ycalc) for the synthesized samples.

To confirm the existence of a single phase and to assess the influence of substituting Ca sites with Cu and Fe in the crystalline structure, Rietveld refinement was performed using the FullProf software. The refinement was based on the experimental crystallographic data Wilson et al., 1999 [9], used as the initial estimate for the unit cell's lattice parameters and atomic occupancy factor. The diffractograms generated through Rietveld refinement (Ycal) and the difference between the observed and calculated data (Yobs-Ycal) are also shown in Figure 1. In Rietveld refinement, the Bragg factor values are minimized, with the low values ranging between 2.95 and 3.35. These results indicate good compatibility between the synthesized structures and the initial estimate for the samples before activation. The agreement between the experimental diffractograms suggests that Cu and Fe were successfully incorporated into the hydroxyapatite crystalline structure by occupying the available calcium sites without the significant formation of a new phase. However, after activation via sulfidation, de XRD patterns of the 12.6CuxSyHap and 15FexSyHap samples displayed small peaks at 2θ~29, 37^0, 59^0, and 64^0, which can be attributed to copper and iron sulfide [8,10].

3.2 Adsorption evaluation

The adsorption capacity of 12.6CuxSyHap, 8FexSyHap, and 15FexSyHap adsorbents, are shown in Figure 2. These results indicate that calcium hydroxyapatite exhibits a lower Hg^0 adsorption capacity, in contrast with Cu and Fe-modified hydroxyapatite performance due to the active iron and copper sulfide sites.

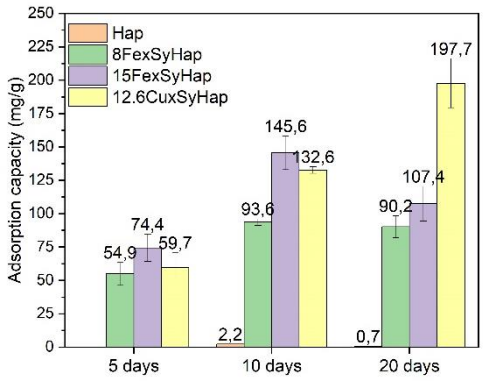

Figure 2. The adsorption capacity for synthesized adsorbents, Hap, 8FexSyHap, 15FexSyHap, and 12.6CuxSyHap

Moreover, no significant variation in the adsorption capacity of 15FexSyHap - 145.6 mg/g - was observed after 10 days, with a similar trend for the 8FexSyHap sample, indicating that adsorption equilibrium had been reached for these adsorbents. In contrast, the 12.6CuxSyHap sample demonstrated a notable increase in adsorption capacity between 10 and 20 days, rising from 132.6 to 197.7 mg/g. Furthermore, the higher adsorption capacity per metal content, 1568.7 mg Hg/g Cu for 12.6CuxSyHap versus 970.5 mg Hg/g Fe for 15FexSyHap, reinforces significant differences in

the physicochemical properties of the two adsorbents.

These results could be explained by differences in morphologies or other physicochemical properties, like active phase dispersion, which facilitates Hg^0 adsorption or bulk diffusion in copper sulfides/hydroxyapatites adsorbents, as Camargo et al. [5] proposed.

Finally, it is noteworthy that the adsorbents synthesized in this study exhibit a markedly higher adsorption capacity compared to other metal sulfides reported in the literature: CuxSyHap: 33.9 mg/g [6]; CuS: 86.22 mg/g [12]; and FeS2/TiO2: 25.1 mg/g [13].

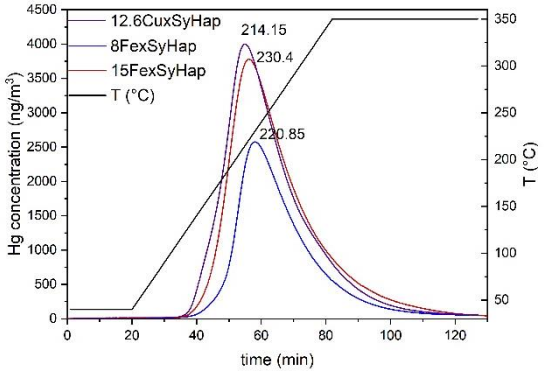

Figure 3. Hg-TPD profiles of Hg° adsorbed on 12.6CuxSyHap, 8FexSyHap, and 15FexSyHap.

The results obtained from mercury temperature-programmed desorption, shown in Figure 3, indicate that all adsorbents immobilized mercury up to approximately 105–110 °C, effectively preventing reemission and ensuring safe disposal.

4. Conclusions

All prepared adsorbents exhibited high performance, with 12.6CuxSyHap and 15FexSyHap achieving adsorption capacities of 197.7 mg/g and 145.6 mg/g, respectively. This demonstrates the effectiveness of dispersing copper and iron sulfides within a hydroxyapatite matrix. The rapid attainment of thermodynamic equilibrium for iron sulfide adsorbents and the markedly superior adsorption capacity of copper sulfide adsorbents can be attributed to differences in dispersion, electronic properties of metal sulfides, and morphology. Furthermore, all synthesized adsorbents effectively immobilize mercury up to 110 °C, preventing atmospheric reemission

Acknowledgments

These authors thank the financial support of CAPES, Carlos Chagas Filho Research Support Foundation of Rio de Janeiro State (FAPERJ), and LABNANO/CBPF for technical support during electron microscopy analysis.

References

[1] M.E. Crespo-Lopez, M. Augusto-Oliveira, A. Lopes-Araújo, L. Santos-Sacramento, P. Yuki Takeda, B. de M. Macchi, J.L.M. do Nascimento, C.S.F. Maia, R.R. Lima, G.P. Arrifano, Mercury: What can we learn from the Amazon?, Environ Int 146 (2021) 106223.

[2] D. Liu, C. Li, T. Jia, J. Wu, B. Li, Novel metal sulfide sorbents for elemental mercury capture in flue gas : A review, Fuel 357 (2024) 129829.

[3] UN Environment, Global Mercury Assessment 2018, 2019.

[4] Y. Yang, W. Xu, R. Huang, T. Zhu, J. Song, Enhancement of Hg0 adsorption performance at high temperature using Cu-Zn bimetallic sulfide with elevated thermal stability, Chemical Engineering Journal 431 (2022).

[5] C.L.M. Camargo, V.M.M. Salim, F.W. Tavares, N.S. de Resende, Phenomenological modeling for elemental mercury capture on hydroxyapatite-based adsorbents: An experimental validation, Fuel 225 (2018) 509–518.

[6] D. dos S. Silva, A.E.C. Villegas, R. De Paiva, R. de P.F. Bonfim, V.M.M. Salim, N.S. De Resende, Iron-substituted hydroxyapatite as a potential photocatalyst for selective reduction of CO2 with H2, Journal of CO2 Utilization 63 (2022) 102102.

[7] M. Bahrami, M.J. Amiri, F. Dehkhodaie, Effect of different thermal activation on hydroxyapatite to eliminate mercury from aqueous solutions in continuous adsorption system, Int J Environ Anal Chem 101 (2021) 2150–2170.

[8] J. Zhao, X. Wu, Y. Ma, W. Liu, Z. Li, S. Zhao, Controlled synthesis of CuS with different morphology and pollution control of Hg0 in non-ferrous smelting flue gas, Fuel 351 (2023) 128921.

[9] R.M. Wilson, J.C. Elliott, S.E.P. Dowker, Rietveld refinement of the crystallographic structure of human dental enamel apatites, American Mineralogist 84 (1999) 1406–1414.

[10] Y. Sun, D. Lv, J. Zhou, X. Zhou, Z. Lou, S.A. Baig, X. Xu, Adsorption of mercury (II) from aqueous solutions using FeS and pyrite: A comparative study, Chemosphere 185 (2017) 452–461.